JACS
JOURNAL OF THE AMERICAN CHEMICAL SOCIETY
Article
pubs.acs.org/JACS

Efficient Extraction of Trapped Holes from Colloidal CdS Nanorods

Kaifeng Wu,[†,#] Yongling Du,[*,‡,#] Hua Tang,[†,§] Zheyuan Chen,[†] and Tianquan Lian[*,†]

[†]Department of Chemistry, Emory University, 1515 Dickey Drive, NE, Atlanta, Georgia 30322, United States
[‡]College of Chemistry and Chemical Engineering, Lanzhou University, Lanzhou, Gansu 730000, China
[§]School of Materials Science and Engineering, Jiangsu University, Zhenjiang, Jiangsu 212013, China

Supporting Information

ABSTRACT: Cadmium Sulfide (CdS) nanostructures have been widely applied for solar driven H_2 generations due to its suitable band gap and band edge energetics. For an efficient photoreduction reaction, hole scavenging from CdS needs to compete favorably with many recombination processes. Extensive spectroscopic studies show evidence for hole trapping in CdS nanostructures, which naturally leads the concern of extracting trapped holes from CdS in photocatalytic reactions. Here, we report a study of hole transfer dynamics from colloidal CdS nanorods (NRs) to adsorbed hole acceptor, phenothiazine (PTZ), using transient absorption spectroscopy. We show that >99% of the holes were trapped (with a time constant of 0.73 ps) in free CdS NRs to form a photoinduced transient absorption (PA) feature. In the presence of PTZ, we observed the decay of the PA feature and corresponding formation of oxidized PTZ^+ radicals, providing direct spectroscopic evidence for trapped hole transfer from CdS. The trapped holes were extracted by PTZ in 3.8 ± 1.7 ns (half-life) to form long-lived charge separated states (CdS^--PTZ^+) with a half lifetime of 310 ± 50 ns. This hole transfer time is significantly faster than the slow conduction band electron−trapped hole recombination (half lifetime of 67 ± 1 ns) in free CdS NRs, leading to an extraction efficiency of 94.7 ± 9.0%. Our results show that despite rapid hole trapping in CdS NRs, efficient extraction of trapped holes by electron donors and slow recombination of the resulting charge-separated states can still be achieved to enable efficient photoreduction using CdS nanocrystals.

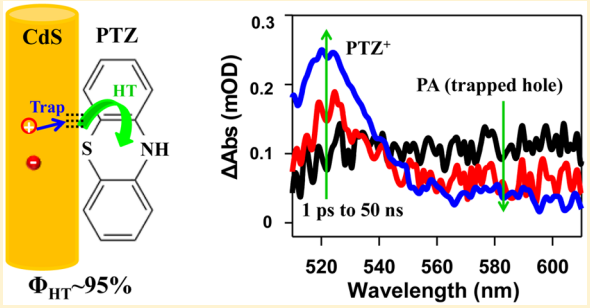

INTRODUCTION

Since Fujishima and Honda's pioneering work of photocatalytic water oxidation using TiO_2 electrode,[1] photodriven water splitting by semiconductors has been extensively investigated.[2] Recent years have seen a particularly drastic resurgence of this field, driven in part by advances in nanomaterial synthesis.[3−6] It is now possible to fabricate nanostructures that can simultaneously have large surface areas for high catalyst loading and small diameters for efficient carrier collection, both of which can in principle enhance photocatalytic performances.[3−6] However, large surface area also increases the probability of electron and hole trapping at surface defect states in nanomaterials, which can potentially lower their photocatalytic performances. This competition between advantages and disadvantages is a common feature for many nanomaterials, including CdS, which has been widely investigated for solar-driven water reduction (H_2 generation) due to its visible light absorption, suitable conduction band (CB) edge energetics, and facile deposition of cocatalysts (such as Pt and Ni nanoparticles) to further enhance its H_2 generation performances.[7−11]

In a typical H_2 generation reaction from CdS nanostructures, photogenerated electron−hole pairs in CdS are separated, with the electron transferred to attached catalysts or active surface sites for proton reduction and hole scavenged by added sacrificial electron donors.[12,13] Although electron transfer processes are often fast (ps to ns time scale),[12−15] consumptions of electrons by catalytic turnover are relatively slow (μs to ms time scale).[16−18] Therefore, for efficient H_2 generation, hole transfer to sacrificial donors needs to be fast to suppress recombinations loss.[12] Indeed, it has recently been demonstrated that hole transfer is the efficiency limiting step in many semiconductor nanostructure based photoreduction systems.[12,19−21] Extensive spectroscopic studies on CdS nanocrystals have revealed that valence band (VB) holes are often trapped into surface states in a subps time scale.[13,22−26] Compared with electron transfer, much less is known about hole transfer from nanocrystals[27−31] and the effect of hole trapping on this process.

Herein, we report the study of hole transfer from colloidal CdS nanorods (NRs) to adsorbed molecular hole acceptors, phenothiazine (PTZ), shown in Scheme 1, using pump−probe transient absorption (TA) spectroscopy on the ps to μs time scale. CdS NR was chosen because previous study reported near unity efficiency of hole trapping,[13] which makes it an excellent model system to investigate trapped hole transfer process. PTZ was used because it is has relatively low oxidation

Received: May 1, 2015
Published: July 29, 2015

DOI: 10.1021/jacs.5b04564
J. Am. Chem. Soc. 2015, 137, 10224−10230

Scheme 1[a]

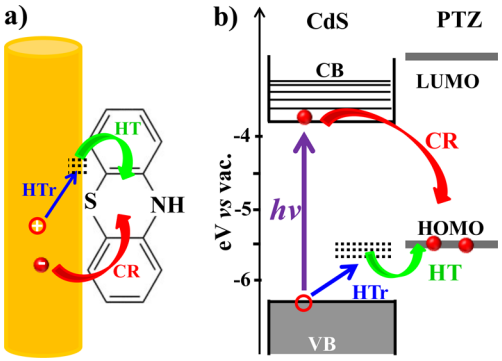

[a](a) Schematic structure of CdS NR-PTZ complexes and possible charge separation and recombination pathways. (b) Energy level scheme of the CdS NR-PTZ complexes and possible exciton quenching pathways. Photoexcited holes can be trapped into mid-gap states (blue arrow) and these trapped holes can transfer to the HOMO of PTZ (green arrow). Charge recombination between electrons in the conduction band of CdS and holes in PTZ HOMO (red arrow) regenerate the ground state complexes.

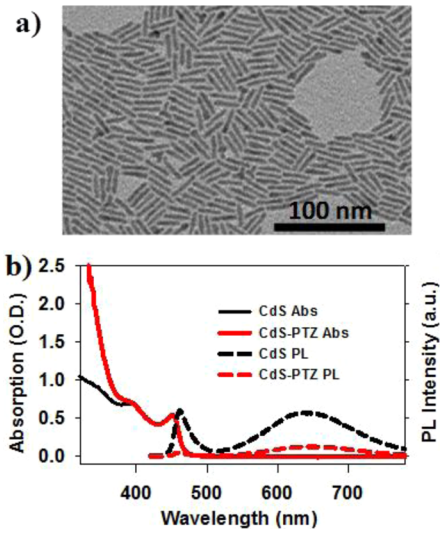

Figure 1. (a) A representative transmission electron microscopy (TEM) image of colloidal CdS NRs. (b) Absorption (solid lines) and photoluminescence (PL, dashed lines) spectra of free CdS NRs (black lines) and CdS NR-PTZ complexes (red lines) dispersed in heptane.

potential (−5.5 V vs vacuum) and its oxidized form, the radical cation (PTZ^+), exhibits a strong and characteristic absorption at ~520 nm,[27] which is well separated from absorption features of CdS NRs. Consistent with previous report, we observed that almost all the holes were trapped (with at time constant of 0.73 ps) in free CdS NRs to form a photoinduced transient absorption (PA) feature. In the presence of PTZ, the trapped holes were transferred to PTZ to form PTZ^+ radical cations in ~3.8 ns (half-life). Compared with a relatively long half lifetime (67 ns) of trapped holes in free CdS NRs, we estimated that an extraction efficiency of ~95% could be achieved. In addition, we showed that charge separated states (CdS^--PTZ+) were long-lived (310 ± 50 ns), which is also highly desirable for efficient photocatalysis.

RESULTS AND DISCUSSION

Sample Preparation and Characterizations. Colloidal CdS NRs were synthesized by a seeded-growth procedure using CdS QDs (diameter of ~2.6 nm) as seeds.[32,33] Synthetic details are described in the Supporting Information (SI). A representative transmission electron microscopy (TEM) image of the as-prepared CdS NRs is shown in Figure 1a. These NRs had average (with standard deviations) length and diameter of 23 (±2.0) nm and 3.5 (±0.2) nm, respectively (Figure S1). Many NRs contained a bulb-like or branched structure near one end with diameter larger than the rod, a common feature in many seeded-grown NRs[14,34−39] Typically, these bulbs surround the seeds, which likely results from imperfect phase control of the CdS seeds: while growth along the [001] crystal axis dominates in wurtzite structure, zinc blende seeds facilitate isotropic growth along several different cryptographic directions.[37] The static absorption and emission spectra of CdS NRs dispersed in heptane are displayed in Figure 1b, exhibiting features similar to previously reported spectra of CdS NRs.[13,33,40] The absorption peaks at ~390 and ~450 nm can be assigned to 1Π and 1Σ excitonic bands, respectively, arising from quantum confinement in the radial direction.[41−43] The photoluminescence (PL) spectrum (measured at 400 nm excitation) shows two distinct bands at around 460 and 650 nm. While the first emission band corresponds well to the Stokes-shifted 1Σ exciton emission, the second one is related to recombination between conduction band (CB) electrons and trapped holes.[13,24,25] The broad width of the latter can be attributed to broad energetic distribution of hole trap levels and/or strong couplings between trapped holes and lattice phonons.[44,45] The PL quantum yield (QY) was estimated to be ~0.1%. Although the band edge and trap emission bands had similar strength (~1:2.8 in area), we will show later that the holes were almost completely (>99.9%) trapped in CdS NRs and it is the extremely low QY of trap emission that leads to comparable strength between these two emissions.

The absorption spectrum of CdS NR-PTZ complexes (Figure 1b) showed CdS exciton peaks similar to free CdS NRs and an additional absorption band of PTZ molecules at <380 nm.[46] Using their extinction coefficients, we estimated that concentration of CdS NRs and PTZ were 8.5×10^{-7} M and 4.2×10^{-3} M, respectively, and their mole ratio was ~1:5000 (see SI for details, Figure S2). The concentration of PTZ was similar to that of sacrificial donors typically used in photocatalytic systems.[20] Since PTZ is soluble in heptane, there exists an equilibrium between PTZ molecules dissolved in heptane and those bound to the NR surfaces. We observed efficient quenching of NR band edge and trap state PL by PTZ (Figure 1b). PL quenching could occur through electron, hole and energy transfer pathways. As shown in Scheme 1b, the energy level alignment between CdS NRs and PTZ only allows hole transfer from the photoexcited CdS to PTZ HOMO, which is followed by subsequent electron transfer from the CdS CB to the oxidized PTZ to regenerate the complex in the ground state. We note that similar hole transfer induced PL quenching using other electron donors, such as thiols, has been previously reported.[12,19] However, PTZ has a spectroscopic feature in the oxidized state (PTZ^+) that allows us to investigate the competition of hole trapping and interfacial transfer dynamics using pump−probe TA spectroscopy.

Ultrafast TA Spectroscopic Studies. The details of pump−probe TA set-ups are described in the SI. Briefly, a pump pulse at 400 nm (~150 fs) was used to selectively excite

DOI: 10.1021/jacs.5b04564
J. Am. Chem. Soc. 2015, 137, 10224−10230

the CdS NRs and the induced absorption changes, as a function of both wavelength and time, were monitored by a white light continuum probe pulse variably delayed (from fs to μs) with respect to the pump pulse, providing a complete record of hole trapping, transfer and recombination events.

Hole Trapping in CdS NRs. The TA spectra of free CdS NRs dispersed in heptane at indicated time delays after 400 nm excitation are shown in Figure 2a. They show a dominant

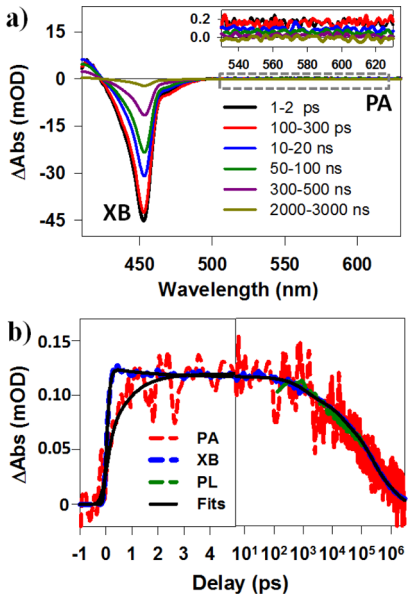

Figure 2. TA spectra and kinetics of CdS NRs measured with 400 nm excitation. (a) TA spectra of CdS NRs at indicated delays, showing a dominant exciton bleach (XB) signal. Inset is a zoom-in of the weak photoinduced absorption (PA) signal. (b) Kinetics of transient PA (red dashed line) and XB (blue dashed line) in NRs and time-resolved PL decay (green dashed line). The black solid lines are multi-exponential fits to these kinetics.

exciton bleach (XB) feature at ~450 nm (that can be assigned to state filling of CB $1\sigma_e$ electronic level of CdS NRs[13]) and an absorptive feature to the blue of XB due to exciton−exciton interactions (i.e., the presence of 1Σ exciton shifts the transition of higher 1Π exciton through Stark Effect).[47] There is also a bleach at ~470 nm, on the red shoulder of XB feature, caused by electrons localized in the bulb region of NRs where the lowest exciton transition is red-shifted from the rod.[14] In our measurement we have used low excitation flux to ensure that the average exciton number on each NR was less than one. This is confirmed by negligible (<11%) XB decay in 1 ns, excluding the existence of multiexciton annihilation process which typically occurs on the several to 100s of ps time scale.[48] The TA spectra also contain a weak broad band photoinduced absorption (PA) feature to the red of XB (with amplitude ~200 times weaker than XB feature). Similar PA features have been observed in other QDs and NRs and were attributed to holes,[13,27,49−52] and hole transfer induced PA decay was reported for CdSe QDs.[27] PA features should be forbidden in ideal nanocrystals, but it can gain some oscillator strengths due to either the presence of surface states or deviation from symmetric nanocrystal shapes.[53]

The kinetics of XB from 0 ps to 3 μs in free CdS NRs is shown in Figure 2b. It is formed in 70(±20) fs due to electron relaxation from $1\pi_e$ to $1\sigma_e$ electronic level. After a slight decay (~5%) within the first 2 ps, the XB feature is long-lived, whose multiexponential fit reveals a half-life of 67 ± 1 ns (amplitude-weighted averaged lifetime of 360 ± 15 ns). The fitting parameters are listed in Table S1 in the SI. This CB electron lifetime is an order of magnitude longer than that in typical quantum confined nanocrystal (~10 ns),[48] suggesting slow electron trapping (well-passivated NRs surfaces) and slow electron−hole radiative and/or nonradiative recombinations. The initial XB bleach (or CB electron) decay within 2 ps (~5%) can be attributed mainly to electron localization from the CdS rod into bulb region in some of the nonuniform NRs driven by confinement energy gradient[14] (see SI for details).

The kinetics of PA feature is wavelength independent from 540 to 720 nm (Figure S3) and in Figure 2b we show the average PA kinetics between 540 and 600 nm. It has a single-exponential (0.73 ± 0.07 ps time constant) formation process slower than that of XB, consistent with previous observations.[13,54] PA decays in exactly the same way as XB and they agree with the PL decay kinetics of the trap emission band. Note that due to the instrument response function (IRF) of our PL decay measurements, we were unable to resolved trap PL decay kinetics before ~200 ps. Nonetheless, the excellent agreement between XB, PA and trap PL indicates that majority of the holes are trapped to form the PA signal and CB electrons decay through recombination with trapped holes. Assuming that band edge electron−hole recombination time is on the order of ~1 ns[13,41] and all the NRs have the ultrafast hole trapping pathway, the percentage of trapped holes is estimated to be ~99.9%. The reduced wave function overlap between the CB electrons and localized trapped holes likely leads to phonon-assisted recombination process with extremely low emission QY and long lifetime. Although the radiative recombination between CB electrons and VB holes is only a minor pathway because of the fast VB hole trapping process, the relatively large radiative decay rates in one-dimensional nanostructures can still lead to appreciable band edge emission in the static PL spectrum. It is comparable to the dominant CB electron-trapped hole recombination process, which decays mainly through nonradiative pathway.[41,55]

Hole Transfer from CdS NRs. CdS NR-PTZ complexes dispersed in heptane were studied under the same conditions (same absorbance at 400 nm and pump power) as free CdS NRs to allow direct comparison of TA signal amplitudes. Compared to free NRs, the TA spectra of NR-PTZ complexes (Figure 3a) are still dominated by a long-lived XB feature, indicating that addition of PTZ neither introduces electron transfer channel nor affected the surface passivation of NRs. As shown in Scheme 1a, PTZ molecules presumably bind to NR surfaces through the sulfur atom due to its strong binding energy with Cd^{2+} on surfaces,[56] by either filling in uncoordinated sites or replacing native phosphonic acid ligands, neither of which should decrease the passivation of Cd^{2+} related electron trap sites. The PA signal (Figure 3b) shows a fast decay on the ~1 ns time scale and a concomitant formation of an absorptive band of oxidized form of PTZ (i.e., PTZ^+ radical) at ~520 nm,[27] providing direct evidence for transfer of trapped holes from CdS NRs to the adsorbed PTZ molecules. The radical signal reaches its maximum at ~100 ns, indicating completion of the hole transfer (HT) process, and decays on the μs time scale, due to charge recombination (CR) between the CdS CB electrons and PTZ^+ radicals (see eq 1).

DOI: 10.1021/jacs.5b04564
J. Am. Chem. Soc. 2015, 137, 10224−10230

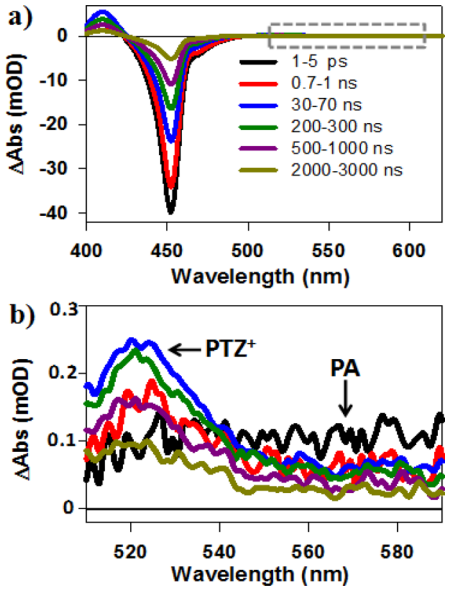

Figure 3. TA spectra of CdS NR-PTZ complexes measured with 400 nm excitation. (a) TA spectra evolution from 1 ps to 3000 ns. (b) Zoom-in of the 500−600 nm wavelength range shows the formation and decay of oxidized PTZ^+ radical signal.

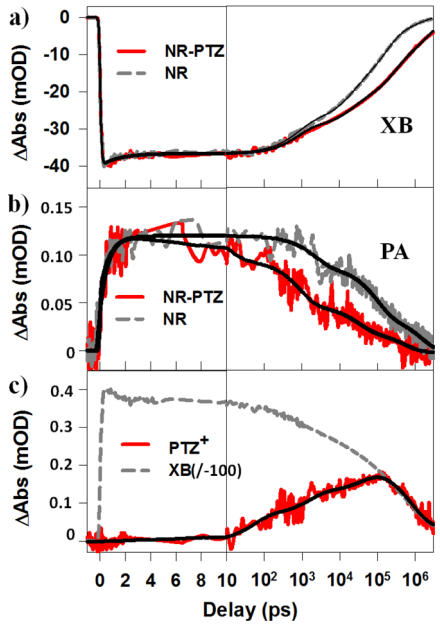

Figure 4. Comparison of TA kinetics of (a) XB and (b) PA in CdS NR-PTZ complexes (red solid lines) and free CdS NRs (gray dashed lines) measured with 400 nm excitation. (c) shows the PTZ^+ radical kinetics (red solid line) and its comparison to XB kinetics (gray dashed line) in CdS NR-PTZ complexes. The black solid lines are multiexponential fits.

$$\begin{aligned} &CdS^*(e-h) - PTZ \\ &\xrightarrow{HT} CdS^-(e) - PTZ^+(h) \\ &\xrightarrow{CR} CdS - PTZ \end{aligned} \quad (1)$$

The charge separation and recombination rates in CdS NR-PTZ complexes can be determined by following the TA kinetics of conduction band electrons (XB), trapped holes (PA) and oxidized hole acceptors (PTZ^+ radical). The fitting model is described in Scheme S1 in the SI. As shown in Figure 4a, the XB feature in CdS NR-PTZ complexes (250 ± 2 ns half lifetime) is longer-lived compared with free NRs (67 ± 1 ns). This is consistent with an interfacial hole transfer process to PTZ, which prolongs CB electron lifetime. The PA in NR-PTZ complexes (Figure 4b) shows the same formation process as in free NRs, indicating that the hole trapping process is not affected by the presence of PTZ. It suggests that in CdS NRs, PTZ does not passivate the hole trap states on NRs and hole transfer to PTZ cannot compete with the intrinsic ultrafast (0.73 ps) hole trapping process. Compared with free NRs, PA signal in NR-PTZ complexes shows much faster decay, with a half-life of 3.6 ± 1.5 ns (average lifetime of 35.8 ± 4.5 ns, Table S1), indicating the transfer of trapped holes to PTZ. The large difference between half and amplitude averaged lifetimes arises from highly heterogeneous nature of hole transfer processes. Since the latter is sensitive to the time constant of slow component which is difficult to be accurately determined,[57−59] we use half-lives to calculate hole transfer time and efficiency according to eqs 2 and 3:

$$1/\tau_{HT} = 1/\tau_{PA,NR-PTZ} - 1/\tau_{PA,NR} \quad (2)$$

$$\Phi_{HT} = \tau_{PA,NR-PTZ}/\tau_{HT} \quad (3)$$

where $\tau_{PA,NR}$ and $\tau_{PA,NR-PTZ}$ are half-lives of PA signals in NRs and NR-PTZ complexes, respectively. The calculated hole transfer time is 3.8 ± 1.7 ns and hole transfer efficiency is 94.7 ± 9.0%. This result suggests that the trapped holes in CdS NRs can still be efficiently extracted, which is crucial for the applications of CdS NRs in photocatalytic reactions.

In addition to the PA signal, hole transfer process was also followed by the kinetics of PTZ^+ radical signal. Due to the overlap of PTZ^+ radical and PA signal at ∼520 nm, the latter was subtracted from the total TA signal at ∼520 nm to obtain the PTZ^+ radical kinetics. Here we have assumed that the PA signal is constant over 500−650 nm spectral window in CdS-PTZ complexes because of the near constant PA amplitudes observed in free NRs (Figure 2a). Fitting the radical kinetics (Figure 4c) by multiexponential formation and decay showed a formation and decay time (half-life) of 4.4 ± 1.2 ns and 310 ± 50 ns. The formation time agrees well with the hole transfer time determined from the PA kinetics. The radical decay process corresponds to the charge recombination between electrons in the CB of CdS NR and holes in PTZ^+ radical to regenerate the CdS NR-PTZ complexes in the ground state. Therefore, PTZ^+ radical and XB show the same decay kinetics when normalized at long delay times (Figure 4c). The amplitude weighted decay time constants of PTZ+ radical (310 ± 50 ns) and XB (250 ± 2 ns) indeed agree with each other within fitting errors. These traces differ at earlier delay time when the PTZ+ radical kinetics contains the contributions of both the radical formation and decay processes (Figure S4). Note that PTZ^+ radicals are stable in the oxidized form to enable the study of the charge recombination process. However, for many sacrificial donors used in photocatalysis, oxidation can lead to their irreversible decomposition or transformation to suppress the charge recombination step. Even in this situation, long-lived charge separation is still highly desirable to allow for the completion of the irreversible chemical changes.

It is well-known that charge transfer rates from nanocrystals increase with the number of adsorbed molecules.[60−62] To

DOI: 10.1021/jacs.5b04564
J. Am. Chem. Soc. 2015, 137, 10224−10230

estimate the number of PTZ per CdS NR (m) and intrinsic hole transfer time per PTZ (τ_{int}), we measured PTZ concentration dependent hole transfer kinetics. Note that in these experiments we used another NR sample that has almost the same average length and diameter as the one used above (Figure S5). As shown in Figure S6, indeed, with increasing PTZ concentration, the PA decay becomes faster. However, PA signal is too small for reliable quantitative analysis of PTZ concentration dependent hole transfer rates. Since we have shown that trapped hole PA decay agrees with trapped state PL decay, we can also use the latter to monitor the hole transfer process. As shown in Figure 5a, trapped state PL decay kinetics

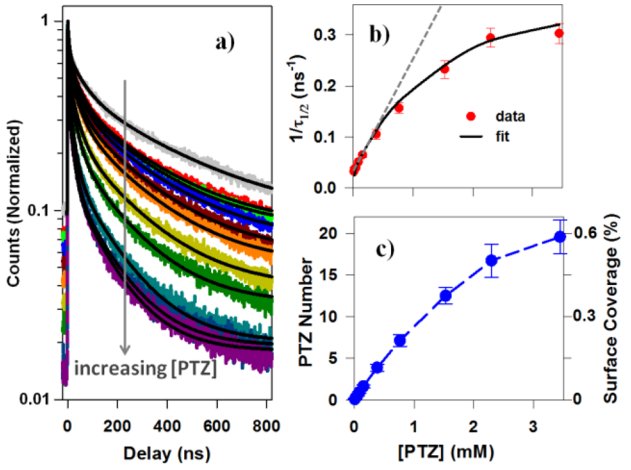

Figure 5. Concentration dependent hole transfer rate. (a) Time-resolved trapped state PL decay kinetics of CdS NRs as a function of PTZ concentration. (b) Average PL decay rate (inverse of half-life) as a function of PTZ concentration and its fit to the model described in the SI. The gray dashed line is a linear plot predicted by dynamic quenching. (c) Estimated average PTZ number per NR (m) and fractional surface coverage (θ) of PTZ on NRs using the model described in the SI.

of CdS NRs becomes faster with increasing PTZ concentration from 0.001 to 3.4 mM. The PL decay kinetics can be fit by multiexponential functions from which half-life was determined to represent the PL decay time (Table S2).

Hole transfer could occur through static (to PTZ adsorbed on the NR surface) and dynamic (to free PTZ in solution via collision) pathways.[29] Figure 5b shows that the average PL decay rate (the inverse of PL decay half-life), increases with the PTZ concentration and approaches saturation at high concentrations. This is inconsistent with dynamics quenching which predicts a linear increase of PL decay rate with quencher concentration. Therefore, static quenching dominates in our CdS NR−PTZ system, i.e., hole transfer occurs to PTZ molecules adsorbed on NR surfaces. Weiss and co-workers reported previously that in PbS QD-molecular electron acceptor systems, static and dynamic quenching occur on the ps and μs time scales, respectively.[63] The dynamic quenching was ~1000 fold slower than diffusion limited rate and was attributed to the presence of native ligands on the QD surface. It appears that in CdS NR- PTZ system, hole transfer by dynamic quenching is also much slower than diffusion limit and is too slow to be observed due to a limited excited state lifetime of CdS NRs.

The plot of average PL decay rate as a function of PTZ concentration (Figure 5b) can be fitted to a static quenching model that contains two assumptions (see SI for details): first, the average number of PTZ per NR (m) depends on PTZ concentration according to the Langmuir adsorption isotherm;[62] second, the distribution of adsorbed molecules is Poissonian.[27,61,64] From the fit, we obtain a hole transfer time per PTZ molecule of τ_{int} = 120 ± 20 ns (or half-life of 83 ± 14 ns). This corresponds to an average hole transfer efficiency of 44.6 ± 5.1% for a NR with only one hole acceptor. The fitting also generates parameters for Langmuir adsorption isotherm (SI), from which we can calculate the fractional surface coverage (θ) of PTZ on NRs and average PTZ number per NR (m), as shown in Figure 5c. The correspondence between half-life ($\tau_{1/2}$) and average PTZ number per NR (m) allows us to estimate that for the CdS NR-PTZ sample studied above ($\tau_{1/2}$ = 3.6 ± 1.5 ns), the average number of adsorbed molecules on the NR surface is ~16 ± 7. Therefore, the high hole transfer efficiency is achieved by the presence of many adsorbed hole acceptors through a static quenching mechanism. Nonetheless, in photocatalytic systems, the concentration of sacrificial donors typically lies within mM to M,[20] under which conditions hole transfer rates are most likely enhanced by the availability of multiple hole transfer acceptors.

Because CB electrons in CdS NRs are long-lived, the red-shifted (~0.75 eV) trap emission band (Figure 1b) can originate from trapped holes with large trapping energy or strong coupling to phonons (large Huang−Rhys parameter).[44,45] In the former case, the trapped holes locate at around −5.6 V (vs vacuum), as estimated from the VB edge (−6.35 V vs vacuum) of CdS NRs, which have a small (~−0.1 eV) driving force and small reorganization energy for transfer to PTZ (−5.5 V vs vacuum). In the latter case, the transfer of the trapped hole has a larger driving force (−0.1 to −0.7 V) and a larger reorganization energy. According to Marcus theory,[65] both mechanisms lead to large hole transfer barriers and slow hole transfer rates. Fortunately, similar mechanisms also slow down recombination between CB electrons and trapped holes. It is the slow intrinsic CB electron-trapped hole recombination that enables efficient hole extraction by PTZ molecules.

The exact nature of hole trap states in CdS nanostructures remains unclear. Previous research indicates that they likely arise from unpassivated sulfur anions on CdS surfaces,[26] or formation of polarons.[44,45] Hole trapping states are likely universal for CdS and other cadmium chalcogenide nanostructures because most ligands used for nanocrystal synthesis and protection are Lewis bases that are expected to bind to the surface Cd^{2+} sites with minor hole passivation effects. Therefore, implementation of CdS into photocatalytic systems inevitably involves extraction of trapped holes. Our results suggest that ultrafast hole trapping in nanocrystals is actually beneficial for efficient charge separation since holes are immobilized at the trapping sites while electrons can diffuse to the catalytic sites to achieve long-lived electron−hole charge separation. Trapped holes can be efficiently extracted by sacrificial electron donors to enable multiple reductions of catalysts required for light driven H_2 generation.

CONCLUSION

In conclusion, we have studied the efficient transfer of trapped holes from colloidal CdS nanorods (NRs) to adsorbed molecular hole acceptor, phenothiazine. We observed that >99% of VB holes were trapped within 0.73 ps in free CdS NRs to form a photoinduced transient absorption (PA) feature. Recombination between CB electrons and trapped holes

DOI: 10.1021/jacs.5b04564
J. Am. Chem. Soc. 2015, 137, 10224−10230

occurred with an average half-life of ~67 ns. In the presence of PTZ, the trapped holes were transferred to adsorbed PTZ molecules in ~3.8 ns (half-life) to form long-lived charge separated states (CdS^{-}-PTZ^{+}) with an half lifetime of 310 ns. This hole transfer time was considerably faster than the slow CB electron-trapped hole recombination inside CdS NRs, leading to an estimated ~95% hole extraction efficiency in this system. Therefore, trapped holes in CdS NRs can still be efficiently extracted. PTZ concentration dependent hole transfer studies revealed that the high hole transfer efficiency was achieved by the presence of ~16 adsorbed hole acceptors through a static quenching mechanism. Efficient extraction of trapped holes enables the application of CdS NRs for photoreduction half reactions (such as light driven H_2 generation by reduction of water). Our findings offer general mechanistic insights into the working principle of CdS based photocatalytic systems.

■ ASSOCIATED CONTENT

Supporting Information

The Supporting Information is available free of charge on the ACS Publications website at DOI: 10.1021/jacs.5b04564.

Sample synthesis. Transient absorption spectroscopy set-ups, kinetics fitting, and PTZ concentration dependent studies. (PDF)

■ AUTHOR INFORMATION

Corresponding Authors

*duyl@lzu.edu.cn

*tlian@emory.edu

Author Contributions

#K. Wu and Y. Du contributed equally to this paper.

Notes

The authors declare no competing financial interest.

■ ACKNOWLEDGMENTS

We gratefully acknowledge the financial support from the Office of Basic Energy Sciences of the US Department of Energy (Grant No. DE-FG02-12ER16347).

■ REFERENCES

(1) Fujishima, A.; Honda, K. *Nature* **1972**, *238*, 37−38.

(2) Lewis, N. S.; Nocera, D. G. *Proc. Natl. Acad. Sci. U. S. A.* **2006**, *103*, 15729−15735.

(3) Walter, M. G.; Warren, E. L.; McKone, J. R.; Boettcher, S. W.; Mi, Q.; Santori, E. A.; Lewis, N. S. *Chem. Rev.* **2010**, *110*, 6446−6473.

(4) Kim, D.; Sakimoto, K. K.; Hong, D.; Yang, P. *Angew. Chem., Int. Ed.* **2015**, *54*, 3259−3266.

(5) Chen, X.; Shen, S.; Guo, L.; Mao, S. S. *Chem. Rev.* **2010**, *110*, 6503−6570.

(6) Hisatomi, T.; Kubota, J.; Domen, K. *Chem. Soc. Rev.* **2014**, *43*, 7520−7535.

(7) Buehler, N.; Meier, K.; Reber, J. F. *J. Phys. Chem.* **1984**, *88*, 3261−3268.

(8) Simon, T.; Bouchonville, N.; Berr, M. J.; Vaneski, A.; Adrović, A.; Volbers, D.; Wyrwich, R.; Döblinger, M.; Susha, A. S.; Rogach, A. L.; Jäckel, F.; Stolarczyk, J. K.; Feldmann, J. *Nat. Mater.* **2014**, *13*, 1013−1018.

(9) Bao, N.; Shen, L.; Takata, T.; Domen, K. *Chem. Mater.* **2007**, *20*, 110−117.

(10) Yan, H.; Yang, J.; Ma, G.; Wu, G.; Zong, X.; Lei, Z.; Shi, J.; Li, C. *J. Catal.* **2009**, *266*, 165−168.

(11) Huang, L.; Wang, X.; Yang, J.; Liu, G.; Han, J.; Li, C. *J. Phys. Chem. C* **2013**, *117*, 11584−11591.

(12) Wu, K.; Chen, Z.; Lv, H.; Zhu, H.; Hill, C. L.; Lian, T. *J. Am. Chem. Soc.* **2014**, *136*, 7708−7716.

(13) Wu, K.; Zhu, H.; Liu, Z.; Rodríguez-Córdoba, W.; Lian, T. *J. Am. Chem. Soc.* **2012**, *134*, 10337−10340.

(14) Wu, K.; Rodríguez-Córdoba, W.; Lian, T. *J. Phys. Chem. B* **2014**, *118*, 14062−14069.

(15) O'Connor, T.; Panov, M. S.; Mereshchenko, A.; Tarnovsky, A. N.; Lorek, R.; Perera, D.; Diederich, G.; Lambright, S.; Moroz, P.; Zamkov, M. *ACS Nano* **2012**, *6*, 8156−8165.

(16) Helm, M. L.; Stewart, M. P.; Bullock, R. M.; DuBois, M. R.; DuBois, D. L. *Science* **2011**, *333*, 863−866.

(17) Fihri, A.; Artero, V.; Razavet, M.; Baffert, C.; Leibl, W.; Fontecave, M. *Angew. Chem.* **2008**, *120*, 574−577.

(18) Karunadasa, H. I.; Chang, C. J.; Long, J. R. *Nature* **2010**, *464*, 1329−1333.

(19) Zhu, H.; Song, N.; Lv, H.; Hill, C. L.; Lian, T. *J. Am. Chem. Soc.* **2012**, *134*, 11701−11708.

(20) Berr, M. J.; Wagner, P.; Fischbach, S.; Vaneski, A.; Schneider, J.; Susha, A. S.; Rogach, A. L.; Jackel, F.; Feldmann, J. *Appl. Phys. Lett.* **2012**, *100*, 223903.

(21) Acharya, K. P.; Khnayzer, R. S.; O'Connor, T.; Diederich, G.; Kirsanova, M.; Klinkova, A.; Roth, D.; Kinder, E.; Imboden, M.; Zamkov, M. *Nano Lett.* **2011**, *11*, 2919−2926.

(22) Tachibana, Y.; Umekita, K.; Otsuka, Y.; Kuwabata, S. *J. Phys. Chem. C* **2009**, *113*, 6852−6858.

(23) Klimov, V.; Bolivar, P. H.; Kurz, H. *Phys. Rev. B: Condens. Matter Mater. Phys.* **1996**, *53*, 1463−1467.

(24) Gopidas, K. R.; Bohorquez, M.; Kamat, P. V. *J. Phys. Chem.* **1990**, *94*, 6435−6440.

(25) Haase, M.; Weller, H.; Henglein, A. *J. Phys. Chem.* **1988**, *92*, 4706−4712.

(26) Wei, H. H.-Y.; Evans, C. M.; Swartz, B. D.; Neukirch, A. J.; Young, J.; Prezhdo, O. V.; Krauss, T. D. *Nano Lett.* **2012**, *12*, 4465−4471.

(27) Huang, J. E.; Huang, Z. Q.; Jin, S. Y.; Lian, T. Q. *J. Phys. Chem. C* **2008**, *112*, 19734−19738.

(28) Sykora, M.; Petruska, M. A.; Alstrum-Acevedo, J.; Bezel, I.; Meyer, T. J.; Klimov, V. I. *J. Am. Chem. Soc.* **2006**, *128*, 9984−9985.

(29) Jiang, Z.-J.; Leppert, V.; Kelley, D. F. *J. Phys. Chem. C* **2009**, *113*, 19161−19171.

(30) Ding, T. X.; Olshansky, J. H.; Leone, S. R.; Alivisatos, A. P. *J. Am. Chem. Soc.* **2015**, *137*, 2021−2028.

(31) Sharma, S. N.; Pillai, Z. S.; Kamat, P. V. *J. Phys. Chem. B* **2003**, *107*, 10088−10093.

(32) Talapin, D. V.; Nelson, J. H.; Shevchenko, E. V.; Aloni, S.; Sadtler, B.; Alivisatos, A. P. *Nano Lett.* **2007**, *7*, 2951−2959.

(33) Carbone, L.; Nobile, C.; De Giorgi, M.; Sala, F. D.; Morello, G.; Pompa, P.; Hytch, M.; Snoeck, E.; Fiore, A.; Franchini, I. R.; Nadasan, M.; Silvestre, A. F.; Chiodo, L.; Kudera, S.; Cingolani, R.; Krahne, R.; Manna, L. *Nano Lett.* **2007**, *7*, 2942−2950.

(34) Khon, E.; Mereshchenko, A.; Tarnovsky, A. N.; Acharya, K.; Klinkova, A.; Hewa-Kasakarage, N. N.; Nemitz, I.; Zamkov, M. *Nano Lett.* **2011**, *11*, 1792−1799.

(35) She, C.; Demortièere, A.; Shevchenko, E. V.; Pelton, M. *J. Phys. Chem. Lett.* **2011**, *2*, 1469−1475.

(36) Lupo, M. G.; Della Sala, F.; Carbone, L.; Zavelani-Rossi, M.; Fiore, A.; Lüer, L.; Polli, D.; Cingolani, R.; Manna, L.; Lanzani, G. *Nano Lett.* **2008**, *8*, 4582-−4587.

(37) Borys, N. J.; Walter, M. J.; Huang, J.; Talapin, D. V.; Lupton, J. M. *Science* **2010**, *330*, 1371−1374.

(38) Hewa-Kasakarage, N. N.; Kirsanova, M.; Nemchinov, A.; Schmall, N.; El-Khoury, P. Z.; Tarnovsky, A. N.; Zamkov, M. *J. Am. Chem. Soc.* **2009**, *131*, 1328−1334.

(39) O'Connor, T.; Panov, M. S.; Mereshchenko, A.; Tarnovsky, A. N.; Lorek, R.; Perera, D.; Diederich, G.; Lambright, S.; Moroz, P.; Zamkov, M. *ACS Nano* **2012**, *6*, 8156−8165.

(40) Saunders, A. E.; Ghezelbash, A.; Sood, P.; Korgel, B. A. *Langmuir* **2008**, *24*, 9043−9049.

(41) Shabaev, A.; Efros, A. L. *Nano Lett.* **2004**, *4*, 1821−1825.

DOI: 10.1021/jacs.5b04564
J. Am. Chem. Soc. 2015, 137, 10224−10230

(42) Bartnik, A. C.; Efros, A. L.; Koh, W. K.; Murray, C. B.; Wise, F. W. *Phys. Rev. B: Condens. Matter Mater. Phys.* **2010**, *82*, 19531301−19531316.
(43) Vietmeyer, F.; McDonald, M. P.; Kuno, M. *J. Phys. Chem. C* **2012**, *116*, 12379−12396.
(44) Mooney, J.; Krause, M. M.; Saari, J. I.; Kambhampati, P. *J. Chem. Phys.* **2013**, *138*, 2047051−2047059.
(45) Mooney, J.; Krause, M. M.; Saari, J. I.; Kambhampati, P. *Phys. Rev. B: Condens. Matter Mater. Phys.* **2013**, *87*, 0812011−0812015.
(46) Ghosh, H.; Sapre, A.; Palit, D.; Mittal, J. *J. Phys. Chem. B* **1997**, *101*, 2315−2320.
(47) Klimov, V. I. *J. Phys. Chem. B* **2000**, *104*, 6112−6123.
(48) Klimov, V. I. *Annu. Rev. Phys. Chem.* **2007**, *58*, 635−673.
(49) Zhu, H.; Lian, T. *J. Am. Chem. Soc.* **2012**, *134*, 11289−11297.
(50) Zhu, H.; Lian, T. *Energy Environ. Sci.* **2012**, *5*, 9406−9418.
(51) Wu, K.; Liu, Z.; Zhu, H.; Lian, T. *J. Phys. Chem. A* **2013**, *117*, 6362−6372.
(52) Wu, K.; Song, N.; Liu, Z.; Zhu, H.; Rodríguez-Córdoba, W.; Lian, T. *J. Phys. Chem. A* **2013**, *117*, 7561−7570.
(53) Tyagi, P.; Kambhampati, P. *J. Chem. Phys.* **2011**, *134*, 094706−094710.
(54) Wu, K.; Rodríguez-Córdoba, W. E.; Yang, Y.; Lian, T. *Nano Lett.* **2013**, *13*, 5255−5263.
(55) Persson, M. P.; Xu, H. Q. *Nano Lett.* **2004**, *4*, 2409−2414.
(56) Aldana, J.; Lavelle, N.; Wang, Y.; Peng, X. *J. Am. Chem. Soc.* **2005**, *127*, 2496−2504.
(57) Guo, J. C.; She, C. X.; Lian, T. Q. *J. Phys. Chem. C* **2007**, *111*, 8979−8987.
(58) She, C.; Anderson, N. A.; Guo, J.; Liu, F.; Goh, W.-H.; Chen, D.-T.; Mohler, D. L.; Tian, Z.-Q.; Hupp, J. T.; Lian, T. *J. Phys. Chem. B* **2005**, *109*, 19345−19355.
(59) Barzykin, A. V.; Tachiya, M. *J. Phys. Chem. B* **2002**, *106*, 4356−4363.
(60) Boulesbaa, A.; Issac, A.; Stockwell, D.; Huang, Z.; Huang, J.; Guo, J.; Lian, T. *J. Am. Chem. Soc.* **2007**, *129*, 15132−15133.
(61) Song, N.; Zhu, H.; Jin, S.; Zhan, W.; Lian, T. *ACS Nano* **2010**, *5*, 613−621.
(62) Morris-Cohen, A. J.; Frederick, M. T.; Cass, L. C.; Weiss, E. A. *J. Am. Chem. Soc.* **2011**, *133*, 10146−10154.
(63) Knowles, K. E.; Malicki, M.; Weiss, E. A. *J. Am. Chem. Soc.* **2012**, *134*, 12470−12473.
(64) Song, N.; Zhu, H.; Jin, S.; Lian, T. *ACS Nano* **2011**, *5*, 8750−8759.
(65) Marcus, R.; Sutin, N. *Biochim. Biophys. Acta, Rev. Bioenerg.* **1985**, *811*, 265−322.

DOI: 10.1021/jacs.5b04564
J. Am. Chem. Soc. 2015, 137, 10224−10230